Ultrasound Image Dataset for Image Analysis Algorithms Evaluation

Camilo Cortes[1,2,3], Luis Kabongo[1,3], Ivan Macia[1,3], Oscar E. Ruiz[2] and Julian Florez[1]

[1]eHealth and Biomedical Applications, Vicomtech-IK4, San Sebastián – Donostia, Spain
{ccortes,lkabongo,imacia,jflorez}@vicomtech.org
[2]Laboratorio de CAD CAM CAE, Universidad EAFIT, Medellín, Colombia
oruiz@eafit.edu.co
[3]Biodonostia Health Research Center, San Sebastián – Donostia, Spain

Abstract. The use of ultrasound (US) imaging as an alternative for real-time computer assisted interventions is increasing. Growing usage of US occurs despite of US lower imaging quality compared to other techniques and its difficulty to be used with image analysis algorithms. On the other hand, it is still difficult to find sufficient data to develop and assess solutions for navigation, registration and reconstruction at medical research level. At present, manually acquired available datasets present significant usability obstacles due to their lack of control of acquisition conditions, which hinders the study and correction of algorithm design parameters. To address these limitations, we present a database of robotically acquired sequences of US images from medical phantoms, ensuring the trajectory, pose and force control of the probe. The acquired dataset is publicly available, and it is specially useful for designing and testing registration and volume reconstruction algorithms.

Keywords: Ultrasound, dataset, registration, reconstruction, data fusion, tracking, verification, validation, evaluation, medical images

1 Introduction

The real-time nature, low-cost and non-invasiveness of US imaging makes it attractive not only for early and simple diagnosis but also more and more as a real-time source of imaging to guide minimally invasive interventions. Nevertheless, due to the poor signal-to-noise ratio that US images present, it is cumbersome to design and test the required image analysis algorithms that are required in patient intra-operative registration, volume reconstruction, data fusion and navigation, among others.

Designing and testing algorithms for image guided interventions require datasets that enable evaluation of their accuracy, performance and sensitivity to design parameters. Ref [1] indicates that public US image datasets are required to evaluate the performance of such algorithms.

adfa, p. 1, 2011.

Most current public US image datasets (e.g. [2, 3]) do not include information of the US *probe* (ultrasound transducer) poses along their acquisition. This means that the images are not spatially tracked, which prevents their use image guided procedures that require spatial information. The scientific community has published some tracked US image datasets ([4], [1]) to address such limitation.

Ref [4] presents US manually-acquired images from brain tumours of patients with the objective of testing US registration algorithms *with respect to* (w.r.t.) Magnetic Resonance Imaging (MRI) scans of the patients. In [1], the CIRS Abdominal Phantom Model 057® is manually scanned with a probe that is tracked with an optical tracking system. Ref. [1] presents US images acquired by varying image acquisition parameters such as frequency, focal depth, gain, power, dynamic range, etc. Although the mentioned data is valuable, manual acquisition of US image datasets implies arbitrary and imprecise control of the pose and force of the sensing device. The consequent variable quality of the image limits the use of these datasets in image guided intervention evaluation environments.

Our Literature Survey in the domain of Ultrasound shows no existing dataset acquired with a machine-controlled, repeatable and systematic manner. Such datasets would be useful for evaluating algorithms for: interventional US registration with preoperative imaging or planning, US registration for automatic annotation and segmentation of reconstructed volumes, US-based navigation based on image fusion or reslicing, US-based planning using volume reconstruction, automatic feature extraction and classification, among others.

The desirable characteristics of a dataset for ultrasound for image analysis algorithms include: (1) Tracked and non-tracked frame captures for random image registration, (2) Reconstructed data for volumetric exploration, (3) Multiple source acquisition for image fusion, (4) Tissue identification and segmentation for modelling and simulation, (5) Intra-scan constant- and variable - quality of acquisition and (6) Ground Truth measurements of targeted areas.

Based on these observations, our contribution aims to produce a public and documented image dataset of medical phantoms containing: a) The complete tracked sequence of robot - acquired US images while the US probe force and pose are precisely controlled, b) Volume reconstruction from the controlled US images, and c) A set of individually tracked US images targeting phantom features (e.g., lesions, anatomical landmarks, etc.) from *ad hoc* poses of the probe (i.e. not considered in item (a)). Geometric specifications of the scanned medical phantoms are available from the providers for comparison and verification purposes.

2 Materials and Methods

2.1 Problem Description

In this section, we state the problem of acquiring sequences of US images along with the poses of the US probe w.r.t. the phantom *coordinate system* (CS). The acquisition methodology of such image dataset allows using it for the evaluation of image analysis algorithms. The hardware required to generate such datasets includes:

(1) a robotic arm, (2) a US machine, (3) an optical tracking system and (4) a set of medical phantoms to be scanned. The goal is to obtain the robotically acquired US image sequences of the medical phantoms by controlling the pose and force of the US probe (). Downstream effects include the repeatability, controllability of such dataset acquisitions. This problem can be formally stated as follows.

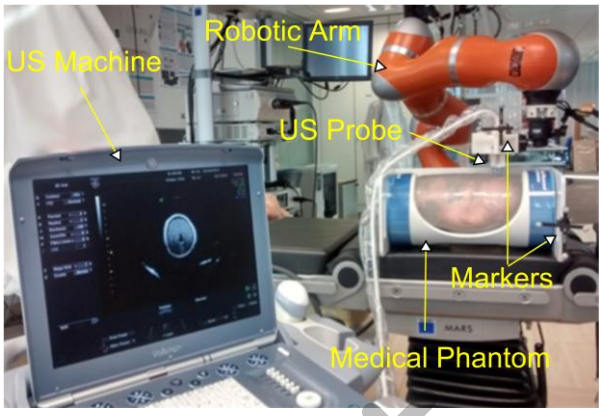

Fig. 1. System to acquire a controlled ultrasound image dataset.

Given:

1. A KUKA LWR IV+ lightweight robot *R* ([5]) able to recreate the dynamics of a spring-damper system with stiffness and damping matrices K and $D \in \Re^{+6x6}$ by using its Cartesian Impedance control ([6]). The desired stiffness and damping along the axes of translation and rotation of the robot task space (*x, y, z, a, b, c*) are indicated by the components of matrices $K = diag\{k_x, k_{y,} k_z, k_{a,} k_b, k_c\}$ and $D = diag\{d_x, d_{y,} d_z, d_{a,} d_b, d_c\}$. The robot provides estimates of the force and torque that is being exerted at the tip of the *Robot End-Effector or tool* (REE).
2. A NDI Polaris Spectra *Optical Tracking System* (OTS) *O* that estimates the pose of a set of arrays of passive markers $A = \{a_0, \cdots, a_g\}$ installed on the desired object to track. The OTS *O* computes the set $T^O(t) = \{T_0^O(t), \cdots, T_g^O(t)\}$ where each $T_i^O(t)$ is a matrix $\in \Re^{4x4}$ that describes the pose of markers $a_i (\in [0, g])$ w.r.t. the *O* reference CS.
3. An ultrasound scanning machine GE Voluson i® with probe *P* (model 9L-RS), which produces a sequence of 2D greyscale images I_i of the region scanned by *P*.
4. A set of medical phantoms $M = \{m_0, \cdots, m_h\}$ that are US-compatible and mimic the physical properties of various tissues and organs of human bodies. A cylindrical hull bounds the *baby phantom* (BP) and a rectangular prism bounds the *abdominal phantom* (AP). Both phantoms are manufactured by CIRS®.

Goal:
A set $H = \{h_0, \cdots, h_n\}$ of tracked US images $h_i = [I_i, T_P^{ref}{}_i]$ for each of the m_j phantoms acquired under pose and force control of *P*. The tracked image $h_i = [I_i, T_P^{ref}{}_i]$ consists of an US image I_i plus a transformation matrix $T_P^{ref}{}_i$, which describes the pose of *P* w.r.t. a reference CS defined by the CS of a marker a_j attached to the m_j scanned medical phantom.

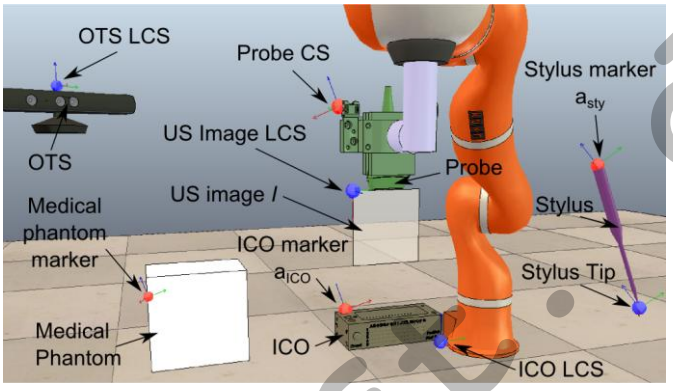

Fig. 2. Schematic diagram of the objects and CS involved in the US image calibration and acquisition procedures. Red CS represent marker a_i CS and blue CS represent local coordinate systems.

2.2 Ultrasound Image Calibration, Acquisition and Processing

In order to calibrate, capture and process the US images, we have used the software PLUS (Public software Library for Ultrasound imaging research) ([7]). Before acquiring the tracked US images, it is necessary to find the transformation T_I^P that relates the CS of the US image *I* w.r.t. the marker attached to the US probe *P* to track it. Knowing T_I^P enables the computation of the 3D position of each of the pixels of the US images of the dataset. Finding T_I^P requires the steps described in the following calibration section. depicts a schematic diagram of the objects and coordinate systems involved in the calibration and acquisition procedures.

Calibration. The calibration procedures are described in detail in [7], and therefore, we briefly discuss them here:

1. Time Axis Calibration: Estimates the time offsets between the data streams provided by the OTS and the US machine. This calibration allows relating US image I_i with the corresponding $T_P^{ref}{}_i$ pose.

2. Stylus Tip Computation: Estimates the transformation $T_{tip}^{a_{sty}}$ of the stylus (narrow elongated rod with a sharp tip) tip w.r.t. the marker a_{sty} CS installed on the stylus to track it. This calibration is necessary to measure the stylus tip coordinates (translation component of T_{tip}^{ref}) w.r.t. a reference CS defined by a marker a_i.
3. Image Calibration Object and OTS Registration: Estimates the transformation $T_{ico}^{a_{ico}}$ of the image calibration object (ICO) *Local CS* (LCS) w.r.t. the CS of marker a_{ico} installed on the ICO to track it. $T_{ico}^{a_{ico}}$ is computed by using a landmark-based registration method using the stylus. Knowing $T_{ico}^{a_{ico}}$ allows expressing the coordinates of the ICO calibration fiducials (N-shaped patterns formed by nylon wires) w.r.t. the OTS, which is a precondition to compute T_I^P.
4. US Image and OTS Registration: Estimates the rigid transformation T_I^P that relates: (a) the coordinates of the ICO fiducials observed in images I_i with (b) the known coordinates of the ICO fiducials w.r.t. the *P* CS (). The details of this algorithm are described in [8].

Image Acquisition Parameters. The ultrasound machine has been configured with the following image acquisition parameters: Receiver frequency=12.00-2.5 MHz (penetration mode), Depth= 14 cm, Focal Points=1, Gain=0.

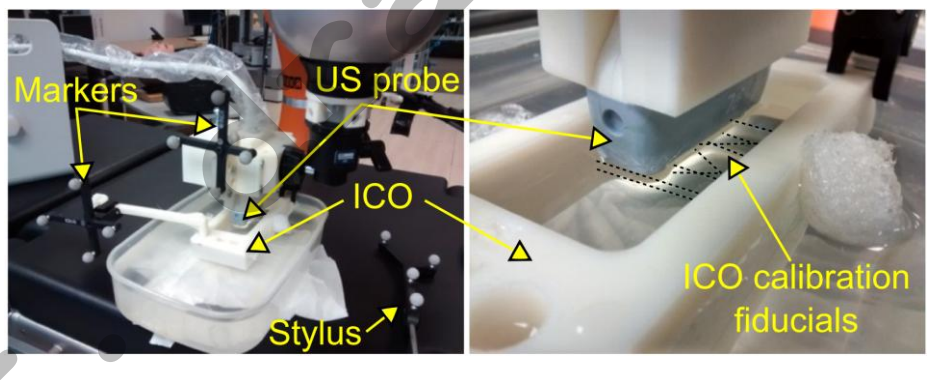

Fig. 3. Registration of the US image CS with respect to the probe CS.

2.3 Motion Control of the Robot

To achieve the desired position-force control of *P* during the robotic-assisted scans, a hybrid position-force controller is implemented on top of the robot Cartesian-Impedance controller. In the force-controlled task subspace of the robot, conditions that allow *P* to keep contact with the surface of the medical phantom are imposed. To

apply the desired force along axis *i* of *R* task space, k_i should be zero and a force set point f_i is commanded along axis *i*. In the position-controlled task subspace, conditions that allow *P* to traverse the region to be scanned are imposed. To control the position along axis *i* of *R* task space, k_i should be assigned with a high magnitude. To guarantee smooth movements, the components of *D* are assigned with high values.

According to the mentioned requirements, we have extended the control module for robot trajectory that we presented in [9] to include force constraints in the desired REE trajectories as follows:

The REE trajectory $E = \{c(\alpha)_0, \cdots, c(\alpha)_b\}$ is composed by a set of parametric curve segments $c(\alpha)$ ($\alpha \in [0,1]$), which keep at least C^0 continuity among themselves. Each $c(\alpha)$ is defined by: (a) The minimum set of poses $Q = \{Q_0, \cdots, Q_s\}$ to define uniquely the desired curve geometry and rotations of the REE, (b) the desired linear velocity $V \in \Re^+$ to go from the initial to the final pose of the segment, and (c) the desired force and torque $\vec{F} \in \Re^6$ to be exerted by the REE while traversing the curve segment.

Prescribed Scanning Trajectories. The BP can be scanned by moving *P* along a straight line parallel to the longitudinal axis of the phantom. The orientation is commanded to keep the probe normal to the phantom surface along the traversed line. The force is commanded to be exerted along the longitudinal axis of *P*. **Table 1** summarizes the features of the trajectories to scan the BP.

Table 1. Features of the desired trajectory to scan the BP (**Fig. 4** left).

Scan	Length (m)	V (m/s)	$norm(\vec{F})$ (N)
1	0,19	0,00100	15
2	0,19	0,00125	15

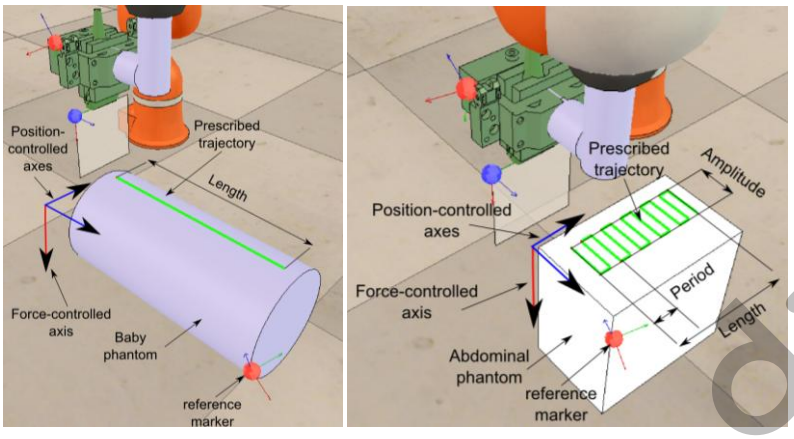

Fig. 4. Left: Prescribed trajectory to scan the BP. Right: Prescribed trajectory to scan the AP.

The AP can be scanned by following a trajectory that resembles a square wave on a plane parallel to the surface of the phantom. The orientation of the REE was programmed to keep the probe normal to be trajectory plane. The force set-point is imposed along the probe longitudinal axis and avoids the deformation of the internal structures of the phantom. **Table 2** summarizes the features of the trajectories to scan the AP.

Table 2. Features of the desired trajectory to scan the AP (**Fig. 4** right)

Scan	Length (m)	Amplitude (m)	Period (m)	V (m/s)	$norm(\vec{F})$ (N)
1	0,15	0,05	0.0375	0,00125	10
2	0,15	0,045	0.03	0,00125	10

3 Results and Discussion

The results corresponding to the US probe and image calibration processes are presented in **Table 3,** and the dataset is publicly available at**:** http:// www.vicomtech.org/demos/us_tracked_dataset/.

Comparing our results with those discussed in reference [7]**,** we conclude that the performed calibrations are suitable to acquire tracked US scans.

With respect to the performance of the implemented hybrid position-force controller, the following metrics are computed to quantify the achievement of the constraints imposed on the trajectories *E* to scan the medical phantoms:

1. The position error metric (PE): is the Hausdorff distance between the prescribed and traversed trajectory of the REE.
2. The average orientation error (AOE): $\mathrm{u} \in \Re^3$ is the representation in exponential map notation ([10]) of the necessary rotation matrix to go from the orientation in

the current REE pose Q_{REE} to the prescribed orientation in pose $Q_i = c(\alpha_i)$ (where α_i represents the parameter value to evaluate $c(\alpha)$). $\|u\|$ is used as a measurement of the REE orientation error. The AOE corresponds to the average of the all the obtained $\|u\|$ while traversing E.

3. The average force error (AFE): is the average magnitude of the difference between desired and exerted force vectors.
4. The average linear velocity error (ALVE): is the average of the differences between the desired and presented linear velocities of the REE. The ALVE metric, does not consider the velocity in the direction of force-controlled axes.

The results of these performance metrics for each scan are presented in **Table 4.**

Table 3. Us Probe Calibration

Calibration:	Result:
Time Axis	Video stream lags 170.7 ms respect to the OTS stream
Stylus Tip Computation	$T_{tip}^{a_{sty}}$ is computed with an average error of 0.378038 mm
ICO and OTS Registration	$T_{ico}^{a_{ico}}$ is computed with an average error of 0.647239 mm
US Image and OTS Registration	T_I^P is computed with an average error of 0.379253 mm

Table 4. Error metrics related to the accomplishment of constraints in E.

Scan	PE (m)	AOE (deg)	AFE (N)	A LVE (m/s)
BP Scan 1	0,00314	0,51620	0,55560	0,00001
BP Scan 2	0,00298	0,50808	0,56241	0,00001
AP Scan 1	0,00368	0,43935	0,65519	0,00004
AP Scan 2	0,00314	0,38477	0,62012	0,00002

From results in **Table 4**, we conclude that the implemented controller allowed scanning the medical phantoms fulfilling the constraints that we imposed on E for each scan.This means that the obtained datasets *H* do present different levels of quality in function of the linear speed (in the case of BP scans) or number of sweeps (in the case of the AP scans) imposed on the trajectory to acquire them.

In addition to the mentioned datasets *H*, we include in our database: (a) volume reconstructions V_H from the *H* datasets generated with the PLUS software (**Fig. 5**) and (b) a set of tracked ultrasound single frames S_M of the various landmarks, organs and lesions that the phantoms present acquired in different poses of the probe with respect to the images in dataset *H*.

These datasets provide ground truth information for testing:

1. Volume reconstruction: Image sequences H can be re-sampled to obtain lower-quality datasets to test (tracked and non-tracked) volume reconstruction algorithms (e.g. volume reconstruction with hole-filling algorithms). In this case, V_H volumes serve as reference reconstructions for quantitative comparison purposes.
2. Registration:
   (a) 3D-2D registrations: Volumes V_H and single tracked images S_M can be used to test 3D-2D registrations. By using T_I^P and T_P^{ref}, the pose T_I^{ref} of an US image I (in S_M) with respect to the reference coordinate system can be computed. Note that T_I^{ref} provides the true transformation between S_M and V_H. Then, the estimated transformation provided by the registration algorithm can be compared to T_I^{ref} in order to measure the registration accuracy.
   (b) 3D-3D registrations: Volumes V_H can be used to test 3D-3D registrations. Regions V_H' can be extracted from V_H, and then, an arbitrary rigid transformation T can be applied to $V_{H.}'$. The registration algorithm should estimate the transformation T.
3. Feature detection: Phantom specifications and volumes V_H can be used as guides to annotate frames in sequences H that contain the desired features to detect. Annotated frames serve as training datasets for feature detection algorithms. Validation can be performed with images S_M or by images obtained by re-slicing $V_{H.}$
4. Segmentation: Phantom-based validation of trained automatic and atlas-based 3D segmentation algorithms using H and V_H.

Fig. 5. Volume rendering in 3D Slicer of the BP (left) and AP (right) of the reconstructed volumes.

4 Conclusions and Future Work

This article presents a public database of sequences of tracked US images in **http://www.vicomtech.org/demos/us_tracked_dataset/** of two medical phantoms that allow the evaluation of image analysis algorithms for procedures such as: patient intra-operatory registration and reconstruction, among others. The methodology proposed to obtain such tracked images consists in using an optical tracking system and a

robot under hybrid position/force control to scan the phantoms along prescribed trajectories of the US probe. We have shown that the constraints that we imposed on the probe trajectories are fulfilled by the proposed system, and therefore, we conclude that the tracked images acquisition was systematic, repeatable and controlled. In this way, the acquired tracked US images overcome the limitations of manually acquired datasets.

This work is an initial approach to provide relevant data for applying image analysis algorithms to ultrasound in interventional context. As an extension to this work a short term contribution will be the acquisition of existing phantoms under CT and MRI for multi-modal reconstruction, fusion and registration. Future work also consists of the automatic generation of trajectories for the robotic scanning of static and dynamic targets.

References

1. V. R. Shivaprabhu, A. Enquobahrie, Z. Mullen, and S. Aylward, "Accelerating ultrasound image analysis research through publically available database," in *SPIE Medical Imaging*, 2013, pp. 867517–867517.
2. S. Balocco, C. Gatta, F. Ciompi, A. Wahle, P. Radeva, S. Carlier, G. Unal, E. Sanidas, J. Mauri, X. Carillo, and others, "Standardized evaluation methodology and reference database for evaluating IVUS image segmentation," *Comput. Med. Imaging Graph.*, vol. 38, no. 2, pp. 70–90, 2014.
3. J. Tian, Y. Wang, J. Huang, C. Ning, H. Wang, Y. Liu, and X. Tang, "The Digital Database for Breast Ultrasound Image," in *11th Joint International Conference on Information Sciences*, 2008.
4. L. Mercier, R. F. Del Maestro, K. Petrecca, D. Araujo, C. Haegelen, and D. L. Collins, "Online database of clinical MR and ultrasound images of brain tumors," *Med. Phys.*, vol. 39, no. 6, pp. 3253–3261, 2012.
5. R. Bischoff, J. Kurth, G. Schreiber, R. Koeppe, A. Albu-Schäffer, A. Beyer, O. Eiberger, S. Haddadin, A. Stemmer, G. Grunwald, and others, "The KUKA-DLR Lightweight Robot arm-a new reference platform for robotics research and manufacturing," in *Robotics (ISR), 2010 41st International Symposium on and 2010 6th German Conference on Robotics (ROBOTIK)*, 2010, pp. 1–8.
6. A. Albu-Schäffer, C. Ott, and G. Hirzinger, "A unified passivity-based control framework for position, torque and impedance control of flexible joint robots," *Int. J. Robot. Res.*, vol. 26, no. 1, pp. 23–39, 2007.
7. A. Lasso, T. Heffter, A. Rankin, C. Pinter, T. Ungi, and G. Fichtinger, "PLUS: Open-source toolkit for ultrasound-guided intervention systems," *IEEE Trans. Biomed. Eng.*, no. 10, pp. 2527–2537, Oct. 2014.
8. G. Carbajal, A. Lasso, Á. Gómez, and G. Fichtinger, "Improving N-wire phantom-based freehand ultrasound calibration," *Int. J. Comput. Assist. Radiol. Surg.*, vol. 8, no. 6, pp. 1063–1072, 2013.
9. C. A. Cortes, I. Barandiaran, O. E. Ruiz, and A. D. Mauro, "Robotic Research Platform For Image-Guided Surgery Assistance," in *Proceedings of the IASTED International Conference Biomedical Engineering (BioMed 2013)*, Innsbruck, Austria, 2013, pp. 427–434.
10. F. S. Grassia, "Practical parameterization of rotations using the exponential map," *J. Graph. Tools*, vol. 3, no. 3, pp. 29–48, 1998.